Functional Tolerance of *Streptomyces* Subtilisin Inhibitor toward Conformational and Stability Changes Caused by Single-Point Mutations in the Hydrophobic Core

Masayuki Oda,[*,1] Atsuo Tamura,[†] Kenji Kanaori,[‡] Shuichi Kojima,[§] Kin-ichiro Miura,[§] Keiko Momma,[∥] Ben'ichiro Tonomura,[∥] and Kazuyuki Akasaka[¶]

[*]Research Institute for Biological Sciences (RIBS), Tokyo University of Science, Noda, Chiba 278-0022; [†]Graduate School of Science and Technology, Kobe University, and PRESTO, JST (Japan Science and Technology Cooperation), Rokkodai-cho, Nada-ku, Kobe 657-8501; [‡]Department of Applied Biology, Kyoto Institute of Technology, Matsugasaki, Sakyo-ku, Kyoto 606-8585; [§]Institute of Biomolecular Science, Gakushuin University, Mejiro-ku, Tokyo 171-8588; [∥]Department of Food Science and Technology, Faculty of Agriculture, Kyoto University, Kitashirakawa, Kyoto 606-8502; and [¶]Department of Biotechnological Science, Faculty of Biology-Oriented Science and Technology, Kinki University, Uchita, Wakayama 649-6493

Single amino acid mutations of Met103 in the hydrophobic core of a serine protease inhibitor, *Streptomyces* subtilisin inhibitor, caused little change in the inhibitory activity, as measured by the inhibitor constant, although some altered the thermodynamic stability of the protein considerably. ^{1}H NMR investigations showed that the conformational stress caused by the replacement of Met103 with Gly, Ala, Val, and Ile, namely, the effects of the cavities generated by replacements with smaller side-chains and of the steric distortions generated by β-branched side-chains, caused considerable changes in the structural arrangement of the side-chains within the core. However, these structural changes were absorbed within the hydrophobic core, without distorting the structure of the reactive site essential for the protein function. These results provide an excellent example of the conformational flexibility of a protein core and the degree of its tolerance of an amino acid replacement. The results also reveal the crucially designed structural relationship between the core of the inhibitor and the enzyme-binding segment with the reactive site in a serine protease inhibitor.

Key words: conformational change, inhibitory function, protein engineering, *Streptomyces* subtilisin inhibitor, thermal stability.

Various strains of *Streptomyces* are known to produce a family of dimeric serine protease inhibitors, called the SSI family inhibitors (*1*). They have a common structural design but consist of a variety of amino acid sequences. The first SSI family inhibitor isolated from *Streptomyces albogriseolus* S-3253, hereafter designated as the wild-type, has a unique homodimeric structure with 11.5-kDa subunits (*2, 3*). The three-dimensional structures of both free SSI and its complex with subtilisin BPN' have been determined (*4–6*). The two subunits face each other through predominantly hydrophobic residues on four-stranded β-sheets, which are tightly bound and make almost a single large hydrophobic core. This arrangement of the two subunits makes the protein quite stable, the wild-type having a thermal transition of over 80°C (*7*). A long protease-binding segment of each subunit, comprising residues Asp68–Tyr75 as a primary binding region, is located on the opposite side of the subunit interface. The middle part of the long binding segment is connected to the core part through a disulfide bridge at residues Cys71 and Cys101. Most of the side chains of the binding segment, containing the reactive site Met73-Val74 at P1-P1', are well exposed to the solvent in a position ready to interact with the target enzymes, such as subtilisin BPN', from which the name originates. Each subunit of SSI strongly binds one protease molecule, and therefore one dimeric SSI molecule binds two enzyme molecules, forming a 2:2 complex. The large hydrophobic core, with the strong contact between the two subunits and the highly exposed reactive-site segments attached to it, makes the protein a unique system to investigate the role of the core in the activity of a globular protein. We approached this system by employing single amino acid substitutions of one central residue, Met103, and determined how each replacement in the tightly packed hydrophobic core of the protein affects both its structure, *e.g.*, the side chain arrangement in the core, and its overall thermodynamic stability. Furthermore, we also analyzed how the replacements in the core part affect the enzyme-binding ability of the protein at the well-exposed reactive-site segment.

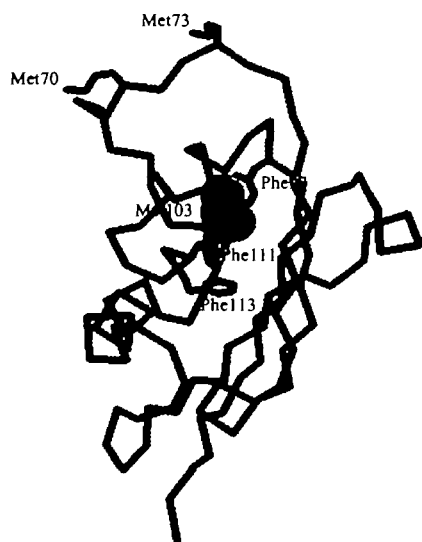SSI contains three methionine residues, which are all

Fig. 1. **Backbone structure of an SSI subunit with the three methionine and three phenylalanine residues, based on the crystallographic coordinates (PDB code, 3SSI).** The side-chain of Met103 is represented as a CPK model, and those of Met70, Met73, Phe97, Phe111, and Phe113 are indicated as stick models.

located at crucial sites for its function and stability. Met73 constitutes the P1 site in the reactive site of the inhibitor, and Met70 constitutes the P4 site of the enzyme-binding segment. Both of the side-chains are well exposed to the solvent, and the motional dynamics of all three Met side-chains have been studied in detail by NMR spectroscopy (*8, 9*). The effects of the Met70 and Met73 mutations of the enzyme-binding segment on the inhibitory activity, stability, and structure of SSI have been studied in some detail (*10–16*). In contrast, Met103 is deeply buried in the hydrophobic core of each subunit and is surrounded by three phenylalanine residues, Phe97, Phe111, and Phe113 (Fig. 1). It is, therefore, located at a crucial position to define the stability of the core. We chose Met103 as the amino acid replacement site, and generated five single mutant proteins, M103G, M103A, M103V, M103L, and M103I, and one double mutant, M73K/M103L. The inhibitory activities were measured for all of the mutants. The conformational rearrangement in the core and the thermal stability changes caused by the mutations were analyzed by ^{1}H NMR and differential scanning calorimetry (DSC), respectively. Together, the results provide a general view of the effect of each hydrophobic core mutation on the structure, the stability, and the function of this protein.

MATERIALS AND METHODS

Protein Preparation—The wild-type SSI was obtained by cultivating *Streptomyces albogriseolus* S-3253, as described previously (*2*). Site-directed mutagenesis was performed by the method of Kojima *et al.* (*10*), and the mutant SSIs were obtained from the culture of the transformed *Streptomyces lividans* 66, as described previously (*17*). The SSI protein secreted into the culture medium was precipitated with ammonium sulfate, then purified by chromatography on an anion exchange column (DE52, Whatman), followed by a gel filtration column (Sephacryl S-200, Amersham Pharma-

cia). The purified proteins were lyophilized and redissolved in an appropriate buffer for analysis. Here the name of each mutant protein is indicated as, for example, M103G for the mutation that replaces Met103 with Gly, and M73K/M103L for the simultaneous mutations that replace Met73 with Lys and Met103 with Leu.

Inhibitor Constant Measurements—The inhibitor constant (K_i) of SSI toward subtilisin BPN' was determined from the residual enzyme activity of subtilisin by using the peptide substrate succinyl-Ala-Ala-Pro-Phe-methyl-coumarylamide, as described previously (*15*). The enzyme activity was analyzed by measuring the fluorescence intensity at 440 nm, with excitation at 350 nm, resulting from the release of 7-amino-4-methyl-coumarin.

NMR Measurements—^{1}H NMR spectra were measured on a JEOL GX-400 spectrometer with standard 5 mm probes. For one-dimensional NMR measurements in the thermal stability experiments, the lyophilized proteins were redissolved to a final protein concentration of 5 mg ml^{-1}. Chemical shifts (δ) were measured relative to an internal reference, sodium 3-trimethylsilylpropionate-2,2,3,3-d$_4$. The midpoint transition temperature for denaturation (T_m) is defined as the temperature at which the peaks of the native and denatured proteins have equal intensities. The van't Hoff enthalpy change for denaturation (ΔH_{vH}) was calculated from the conventional linear van't Hoff plot, using a two-state model for the scheme N$_2$ $\leftrightarrow$ 2D (*18*). For two-dimensional NMR measurements, the protein concentration was 10 mg ml^{-1} in 40 mM sodium deuterated phosphate buffer, pH 7.0, containing 100 mM NaCl. Before NMR measurements, the sample was incubated for 10 min at 70°C to exchange the peptide amide protons for deuteriums. The two-dimensional spectra were measured using phase-sensitive double-quantum filtered correlation spectroscopy (DQF-COSY) (*19, 20*). The spectra were collected into the data points of ω_1 = 256 and ω_2 = 2,048, respectively, with a spectral width of 5,000 Hz. The residual ^{1}H^{2}HO signal was saturated during the recycle time.

DSC Measurements—DSC experiments were carried out on a DASM-4 scanning microcalorimeter. The temperature scanning rate was 1°C min^{-1}. The lyophilized proteins were redissolved in 25 mM sodium phosphate buffer, pH 7.0, containing 100 mM NaCl, in ^{1}H$_2$O or ^{2}H$_2$O. The denaturation temperature in the DSC experiments (T_D) was defined as the temperature where the molar heat capacity is maximal.

RESULTS

Inhibitory Activity—All of the Met103-substituted mutant proteins were overexpressed and purified in amounts sufficient for NMR measurements and biochemical characterizations (Table I). The productivity of the mutant proteins varied considerably, tending to be lower for mutants with smaller side-chains, but it also varied from one preparation to another. The K_i values of the Met103 mutants toward subtilisin BPN' were determined and are summarized in Table I. The inhibitory activities of all of the mutants were surprisingly similar to that of the wild-type SSI.

Thermal Stability—The thermal stabilities of the mutant proteins were analyzed based on the one-dimensional ^{1}H

NMR signals obtained as a function of temperature at pH 7.0. As reported previously (8, 21), the three methyl proton signals of Met70, Met73, and Met103 of the wild-type native SSI are separately observed in the one-dimensional ^{1}H NMR spectrum (Fig. 2A). In the denatured state, the signals of Met73 and Met103 overlap, but the signal of Met70 is separately observed and can be used to monitor the denatured fraction. Based on the respective ^{1}H NMR signals, Met70 and the sum of Met73 and Met103, the T_m and ΔH_{vH} values could be determined from the van't Hoff analysis. The chemical shifts of the Met residues of the mutants were similar to those of the wild-type in both the native and denatured states. In the case of the Met103-substituted mutant protein, the transition for unfolding could be analyzed based on either the Met70 or Met73 signal, respectively (Fig. 2B). In the same way, the transition could be analyzed based on either the Met70 or Met103 signal in the M73K mutant, and on the Met70 signal in the M73K/

M103L mutant. Table II summarizes the thermodynamic parameters of the wild-type and the seven mutant proteins studied at pH 7.0. The T_m values of M103G, M103A, M103V, and M103I were lower than that of the wild-type, while that of M103L was almost the same as that of the wild-type. The invariance of T_m upon the substitution of Met103 with Leu was also noted between M73K/M103L and M73K (Table II).

In order to compare the results in Table II with the thermodynamic parameters obtained in ^{1}H$_2$O in a previous DSC work (22), the solvent isotope effects between ^{1}H$_2$O and ^{2}H$_2$O must be evaluated. Table III summarizes the thermodynamic parameters of the wild-type and M73K proteins in ^{1}H$_2$O and ^{2}H$_2$O, respectively, and M73K/M103L in ^{1}H$_2$O, obtained from DSC measurements. The T_D values of both the wild-type SSI and the M73K mutant in ^{2}H$_2$O

TABLE I. **Yields and inhibitory constants of wild-type SSI and mutant proteins.**

Protein	Hydrophobicity[a] (kcal mol^{-1})	Yield[b] (mg liter^{-1})	K_i[c] (M)
Wild-type	1.68	225.0	$1.8 \pm 0.3 \times 10^{-11d}$
M103G	0	46.8	$1.1 \pm 0.6 \times 10^{-11}$
M103A	0.42	50.3	$0.9 \pm 0.2 \times 10^{-11}$
M103V	1.66	61.0	$2.3 \pm 1.1 \times 10^{-11}$
M103L	2.32	104.3	$1.1 \pm 0.6 \times 10^{-11}$
M103I	2.46	68.4	$2.3 \pm 0.7 \times 10^{-11}$
M73K	1.68	141.7	$1.8 \pm 0.4 \times 10^{-11d}$
M73K/M103L	2.32	85.6	n.d.[e]

[a]Hydrophobicity represents the free energy of transfer of the introduced amino acid into position 103 from octanol to water (31). [b]Yield represents the amount of the protein purified from 1-liter culture. [c]K_i values were calculated based on a nonlinear fitting method (15). [d]Data were taken from Masuda-Momma et al. (15). [e]Not determined.

TABLE II. **Thermodynamic parameters of wild-type SSI and mutant proteins.**

Protein	T_m[a] (°C)	ΔT_m[b] (°C)	ΔH_{vH}[a] (kcal mol^{-1})	T_m[c] (°C)
Wild-type	86.2 ± 0.8	0	177.1 ± 6.8	82.2
M103G	73.6 ± 0.4	−12.6	122.0 ± 7.4	68.6
M103A	82.7 ± 0.9	−3.5	166.5 ± 5.6	78.0
M103V	82.6 ± 1.1	−3.6	147.5 ± 8.9	78.7
M103L	86.2 ± 0.6	0	171.5 ± 14.8	82.5
M103I	83.0 ± 0.6	−3.2	170.1 ± 18.3	78.3
M73K	87.0 ± 0.7	0.8	221.7 ± 23.5	82.9
M73K/M103L	86.9 ± 1.1	0.7	184.3 ± 2.3	n.d.

[a]T_m and ΔH_{vH} are the average values determined from the van't Hoff analysis using the methyl proton signals of methionine residues, as mentioned in "RESULTS." [b]ΔT_m is the change in T_m relative to that of the wild-type. [c]Calorimetric data in ^{1}H$_2$O taken from Tamura et al. (16, 22).
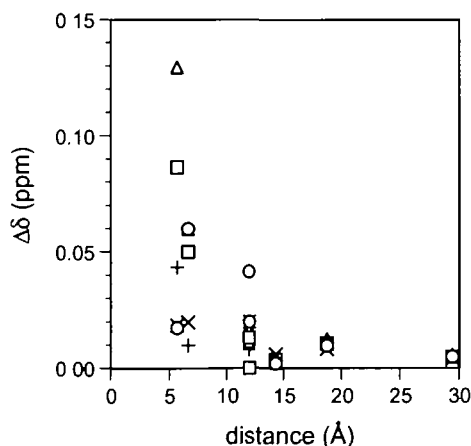
Fig. 3. **Chemical shift differences of the aromatic proton signals between the mutant proteins and the wild-type (Δδ).** The correlation of Δδ with the distance from the substituted site, Met103 (Cβ), to each residue, Phe (Cγ), Tyr (Cγ), Trp (C9), His (C2), calculated from the crystal structure (PDB code, 3SSI) is plotted for M103G (○), M103A (×), M103V (□), M103L (+), and M103I (△). The Δδ values are the average chemical shift differences of the C2, C3, C5, C6 protons for the Phe and Tyr residues, the C4, C5, C6, C7 protons for the Trp residue, and the C2, C4 protons for the His residues in the DQF-COSY spectra, measured at 60°C in 40 mM sodium deuterated phosphate buffer, pH 7.0, containing 100 mM NaCl. The calculated distances are 5.66 Å to Phe111, 6.65 Å to His106, 11.93 Å to Tyr93, 11.98 Å to His43, 14.34 Å to Tyr75, 18.73 Å to Trp86, and 29.42 Å to Tyr7, respectively.
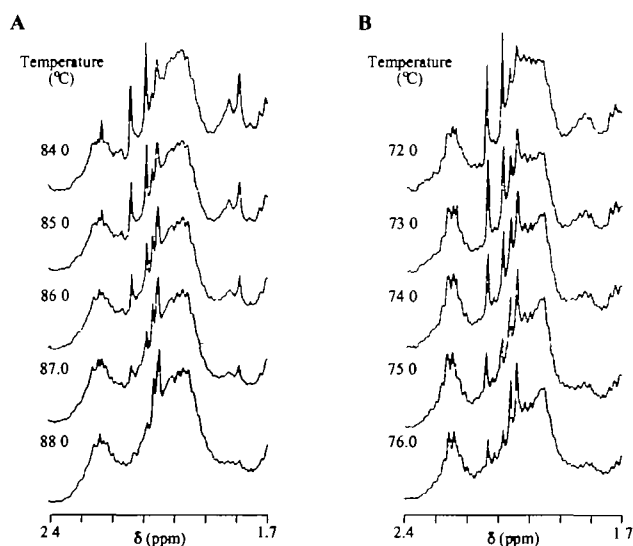

Fig. 2. **Temperature dependence of the ^{1}H NMR spectra of wild-type (a) and M103G (b) in the methyl proton region.** Each signal was previously assigned as follows: Met103 in the native state at δ = 1.78, Met70 in the native state at δ = 2.08, Met73 in the native state at δ = 2.13, Met73 and Met103 in the denatured state at δ = 2.04, and Met70 in the denatured state at δ = 2.06 (8).

were higher than those in ^1H_2O by 3.5°C. The calorimetric enthalpy changes for denaturation (ΔH_{cal}) in ^2H_2O were smaller than those in ^1H_2O. The T_m values obtained from the DSC measurements in ^2H_2O were comparable to those obtained from the NMR measurements (Table II). The thermal stability of M73K/M103L was similar to that of M73K, while that of M73K was slightly higher than that of the wild-type.

Conformational Change—The effects of the Met103 mutations on the conformational change of SSI were analyzed, based on the ^1H chemical shift values of some representative side chains. The methyl proton signals of Met70 and Met73, located at the crucial positions of the reactive-site segment (P1 and P4), showed similar δ and pK_a values among the wild-type and mutant proteins (data not shown), which is consistent with the notion that the mutation does not significantly affect the conformation of the reactive-site segment. These residues are well separated from the mutation site (residue 103): Met70 (16.55 Å away from the Cβ of Met103) and Met73 (14.67 Å). The results are in accordance with the observation that the mutation caused no significant changes in the inhibitor constant (Table I).

In contrast, the residues on the core part of the protein were considerably affected by the mutations. Among the previously assigned aromatic ^1H NMR signals of SSI (*21, 23, 24*), the δ values of the five single-mutant proteins were compared with those of the wild-type in the phase-sensitive DQF-COSY spectra. Figure 3 shows the chemical shift differences of these signals between the mutant proteins and the wild-type (Δδ) at 60°C against the distance between the substituted site and each residue. The Δδ values were smaller in the residues further from the substitution site. On the other hand, the substitution effect was larger for the M103G and M103A mutants than for the others, apparently representing the greater effect of the substitutions with the smaller sized Gly and Ala residues. Although the hydrophobicity of Val is similar to that of Met, this substitution caused a conformational change within the hydrophobic core. In addition, the hydrophobicity of Ile is similar to that of Leu, and the Δδ values of M103I were larger than those of M103L.

DISCUSSION

The present NMR analyses indicated that the cavities generated by Gly and Ala, and the steric distortions generated by the β-branched amino acids, Val and Ile, at position 103 of SSI induce large changes in the Δδ values (Fig. 3). Although the chemical shifts can be affected by various factors, such as the ring current and the solvation effects, the major contribution caused by the mutation should be due to the conformational change, which is mainly attributable to the microenvironmental changes of the three phenylalanine residues surrounding the substituted site. It should be noted that the larger Δδ values were only observed for the residues closer to the substituted site, indicating that the conformational rearrangement is induced within the hydrophobic core, while the conformation outside the hydrophobic core remains almost unchanged. The inhibitory activities of the Met103-substituted mutant proteins also support the results of the local conformational rearrangement. Since the reactive site of SSI is located over 14 Å away from

Met103, its conformation and flexibility are not affected by the substitution. This is in contrast to the mutations of the P1 site in the reactive site, which altered the inhibitory function while causing only a slight conformational change (*15*).

The thermal stability of each mutant protein could be correlated with the extent of the conformational rearrangement in the hydrophobic core (Table II and Fig. 3). The present NMR analyses indicate that the mutational effect in M103G and M103A is due to the newly generated cavity in the hydrophobic core, and that in M103V and M103I is due to steric distortion, both of which cause a conformational rearrangement in the hydrophobic core. The destabilizations of M103G and M103A would also be caused by the increased backbone conformational flexibility in the unfolded state, as mentioned previously (*22*). In contrast, the thermal stability of M103L was almost unchanged, similar to that of M73K/M103L relative to M73K. Although Leu has a γ-branched side-chain and greater hydrophobicity than Met, this mutation would only cause a small conformational change, which would minimally affect the conformational stability at neutral pH (Table II).

Both the present NMR and previous DSC studies yielded similar results for the thermal stabilities of the five single mutant proteins, although relatively higher T_m values were observed in the present analyses (*22*). Several reports have shown the relatively higher stability in ^2H_2O and discussed the solvent isotope effects (*25, 26*). In the case of SSI, the T_m values in ^2H_2O at pH 7.0 analyzed using NMR were 4.3 ± 0.8°C higher than those in ^1H_2O analyzed using DSC (Table II). The present DSC measurements of the wild-type and M73K proteins in ^2H_2O also showed higher T_D values than those obtained in ^1H_2O, and those in ^2H_2O were similar to the T_m values obtained in the NMR measurements (Tables II and III). These results indicate that the present NMR analyses can accurately determine the thermal stability, and the higher T_m values in ^2H_2O for the NMR measurements should be due to the solvent isotope effects. While calorimetric analyses can provide precise thermodynamic parameters, NMR analyses can monitor the transitions of the respective residues. The respective NMR signals of the three methionine residues showed that the unfolding transition of SSI is cooperative.

Some reports have shown that the cavity in the hydrophobic core is needed for the protein function, although the conformational stability of the wild-type is somewhat lower than that of the cavity-filling mutant protein (*27, 28*). The core-packing can affect the conformational flexibility, which is likely to be important for the interactions with other molecules or the enzymatic activity. Consonni *et al.* showed that a single-point mutation in the hydrophobic core causes it to undergo a major conformational rearrangement, resulting in the loss of the protein function and stability (*29*).

TABLE III. **Calorimetric data of wild-type SSI and mutant proteins in ^1H_2O and ^2H_2O.**

Protein	Conc. (mg ml^{-1})	Solvent	T_D (°C)	ΔH_{cal} (kcal mol^{-1})
Wild-type	0.86	^1H_2O	82.8	179.9
Wild-type	1.23	^2H_2O	86.3	162.6
M73K	1.20	^1H_2O	83.9	159.5
M73K	1.42	^2H_2O	87.4	145.3
M73K/M103L	0.94	^1H_2O	83.9	142.4

In contrast, the present structural and thermodynamic analyses using SSI showed that the mutational effects can be accommodated by rearrangements within the hydrophobic core, to maintain its inhibitory activity. This may be a characteristic feature of proteinase inhibitors. Canonical inhibitors of serine proteinases, including SSI, possess an exposed binding loop, and the binding affinity of less stable inhibitor mutants, which are still thermostable, is almost unchanged in the physiological temperature range *(30)*. Although the substitution of Trp86 with His changed SSI into a temporary inhibitor, the inhibitory activity of this mutant protein was similar to that of the wild-type SSI *(21)*. Together with this result, the present study clearly showed that the structural rearrangement caused by single-point mutations in the hydrophobic core can affect the thermal stability, but can also be somewhat absorbed within the hydrophobic core without changing the inhibitory function.

REFERENCES

1. Terabe, M., Kojima, S., Taguchi, S., Momose, H., and Miura, K. (1996) New subtilisin-trypsin inhibitors produced by *Streptomyces*: primary structures and their relationship to other proteinase inhibitors from *Streptomyces*. *Biochim. Biophys. Acta.* **1292**, 233–240
2. Murao, S., Sato, S., and Muto, N. (1972) Isolation of alkaline pretease inhibitor producing microorganisms. *Agric. Biol. Chem.* **36**, 1737–1744
3. Hiromi, K., Akasaka, K., Mitsui, Y., Tonomura, B., and Murao, S. (1985) *Protein Protease Inhibito—The Case of Streptomyces Subtilisin Inhibitor*, Elsevier, Amsterdam
4. Mitsui, Y., Satow, Y., Watanabe, Y., and Iitaka, Y. (1979) Crystal structure of a bacterial protein proteinase inhibitor (*Streptomyces* subtilisin inhibitor) at 2.6 Å resolution. *J. Mol. Biol.* **131**, 697–724
5. Takeuchi, Y., Satow, Y., Nakamura, K.T., and Mitsui, Y. (1991) Refined crystal structure of the complex of subtilisin BPN' and *Streptomyces* subtilisin inhibitor at 1.8 Å resolution. *J. Mol. Biol.* **221**, 309–325
6. Sasakawa, H., Tamura, A., Fujimaki, S., Taguchi, S., and Akasaka, K. (1999) Secondary structures and structural fluctuation in a dimeric protein, *Streptomyces* subtilisin inhibitor. *J. Biochem.* **126**, 859–865
7. Tamura, A., Kojima, S., Miura, K., and Sturtevant, J.M. (1994) Effect of an intersubunit disulfide bond on the stability of *Streptomyces* subtilisin inhibitor. *Biochemistry* **33**, 14512–14520
8. Akasaka, K., Fujii, S., and Hatano, H. (1982) Dynamic states of the three methionyl residues of *Streptomyces* subtilisin inhibitor. ¹H NMR studies. *J. Biochem.* **92**, 591–598
9. Tamura, A., Matsushita, M., Naito, A., Kojima, S., Miura, K., and Akasaka, K. (1996) Dynamics of the three methionyl side chains of *Streptomyces* subtilisin inhibitor. Deuterium NMR studies in solution and in the solid state. *Protein Sci.* **5**, 127–139
10. Kojima, S., Obata, S., Kumagai, I., and Miura, K. (1990) Alteration of the specificity of the *Streptomyces* subtilisin inhibitor by gene engineering. *Bio/Technology* **8**, 449–452
11. Kojima, S., Kumagai, I., and Miura, K. (1990) Effect of inhibitory activity of mutation at reaction site P4 of the *Streptomyces* subtilisin inhibitor, SSI. *Protein Eng.* **3**, 527–530
12. Kojima, S., Nishiyama, Y., Kumagai, I., and Miura, K. (1991) Inhibition of subtilisin BPN' by reaction site P1 mutants of *Streptomyces* subtilisin inhibitor. *J. Biochem.* **109**, 377–382
13. Takeuchi, Y., Noguchi, S., Satow, Y., Kojima, S., Kumagai, I.,

14. Miura, K., Nakamura, K.T., and Mitsui, Y. (1991) Molecular recognition at the active site of subtilisin BPN': crystallographic studies using genetically engineered proteinaceous inhibitor SSI (*Streptomyces* subtilisin inhibitor). *Protein Eng.* **4**, 501–508
15. Takeuchi, Y., Nonaka, T., Nakamura, K.T., Kojima, S., Miura, K., and Mitsui, Y. (1992) Crystal structure of an engineered subtilisin inhibitor complexed with bovine trypsin. *Proc. Natl. Acad. Sci. USA* **89**, 4407–4411
16. Masuda-Momma, K., Hatanaka, T., Inouye, K., Kanaori, K., Tamura, A., Akasaka, K., Kojima, S., Kumagai, I., Miura, K., and Tonomura, B. (1993) Interaction of subtilisin BPN' and recombinant *Streptomyces* subtilisin inhibitors with substituted P₁ site residues. *J. Biochem.* **114**, 553–559
17. Tamura, A. and Sturtevant, J.M. (1995) A thermodynamic study of mutant forms of *Streptomyces* subtilisin inhibitor. III. Replacements of a hyper-exposed residue, Met73. *J. Mol. Biol.* **249**, 646–653
18. Obata, S., Furukubo, S., Kumagai, I., Takahashi, H., and Miura, K. (1989) High-level expression in *Streptomyces lividans* 66 of a gene encoding Streptomyces subtilisin inhibitor from *Streptomyces albogriseolus* S-3253. *J. Biochem.* **105**, 372–376
19. Tamura, A., Kimura, K., and Akasaka, K. (1991) Cold denaturation and heat denaturation of *Streptomyces* subtilisin inhibitor. 2. ¹H NMR studies. *Biochemistry* **30**, 11313–11320
20. Bachmann, P., Aue, W.P., Muller, L., and Ernst, R.R. (1977) Phase separation in two-dimensional spectroscopy. *J. Magn. Reson.* **28**, 29–39
21. States, D.J., Haberkorn, R.A., and Ruben, D.J. (1982) A two-dimensional nuclear Overhauser experiment with pure absorption phase in four quadrants. *J. Magn. Reson.* **48**, 286–292
22. Tamura, A., Kanaori, K., Kojima, S., Kumagai, I., Miura, K., and Akasaka, K. (1991) Mechanisms of temporary inhibition in *Streptomyces* subtilisin inhibitor induced by an amino acid substitution, tryptophan 86 replaced by histidine. *Biochemistry* **30**, 5275–5286
23. Tamura, A. and Sturtevant, J.M. (1995) A thermodynamic study of mutant forms of *Streptomyces* subtilisin inhibitor. I. Hydrophobic replacements at the position of Met103. *J. Mol. Biol.* **249**, 625–635
24. Fujii, S., Akasaka, K., and Hatano, H. (1980) Acid denaturation steps of *Streptomyces* subtilisin inhibitor. A proton magnetic resonance study of individual histidine environment. *J. Biochem.* **88**, 789–796
25. Fujii, S., Akasaka, K., and Hatano, H. (1981) Proton magnetic resonance study of *Streptomyces* subtilisin inhibitor. pH titration and assignments of individual tyrosyl resonances. *Biochemistry* **20**, 518–523
26. Makhatadze, G.I., Clore, G.M., and Gronenborn, A.M. (1995) Solvent isotope effect and protein stability. *Nature Struct. Biol.* **10**, 852–855
27. Kuhlman, B. and Raleigh, D.P. (1998) Global analysis of the thermal and chemical denaturation of the N-terminal domain of the ribosomal protein L9 in H₂O and D₂O. Determination of the thermodynamic parameters, Δ*H°*, Δ*S°*, and Δ*C_p*°, and evaluation of solvent isotope effects. *Protein Sci.* **7**, 2405–2412
28. Oda, M., Furukawa, K., Ogata, K., Sarai, A., Ishii, S., Nishimura, Y., and Nakamura, H. (1997) Identification of indispensable residues for specific DNA-binding in the imperfect tandem repeats of c-Myb R2R3. *Protein Eng.* **10**, 1407–1414
29. Akasako, A., Haruki, M., Oobatake, M., and Kanaya, S. (1997) Conformational stabilities of *Escherichia coli* RNase HI variants with a series of amino acid substitutions at a cavity within the hydrophobic core. *J. Biol. Chem.* **272**, 18686–18693
30. Consonni, R., Santomo, L., Fusi, P., Tortora, P., and Zetta, L. (1999) A single-point mutation in the extreme heat- and pressure-resistant Sso7d protein from *Sulfolobus solfataricus* leads to a major rearrangement of the hydrophobic core. *Biochemistry* **38**, 12709–12717
31. Bode, W. and Huber, R. (1992) Natural protein proteinase inhibitors and their interaction with proteinases. *Eur. J. Biochem.* **204**, 433–451
32. Eisenberg, D. and McLachlan, A.D. (1986) Solvation energy in protein folding and binding. *Nature* **319**, 199–203